

Monolithic Integrated Circuits Incorporating InP-Based Heterostructure Barrier Varactors

T. David, S. Arscott, J.-M. Munier, T. Akalin, P. Mounaix, G. Beaudin, and D. Lippens

Abstract—Fully integrated monolithic circuits incorporating InP-based heterostructure barrier varactor (HBV) frequency multipliers have been fabricated via epitaxial liftoff and transfer-substrate techniques onto a quartz substrate. We have obtained a maximum output power of 6 mW at 288 GHz corresponding to an overall efficiency of 6%. In addition, we have observed a 45-GHz, 3-dB bandwidth centered around 300 GHz for a constant input power of 70 mW.

Index Terms—Epitaxial liftoff, frequency multipliers, heterojunction barrier varactor, millimeter-wave monolithic integrated circuits, transfer-substrate.

I. INTRODUCTION

MODERN telecommunications systems currently require bit-rates in excess of 40 Gbs^{-1} , thus necessitating low-cost, ready-to-use integrated circuitry, incorporating both active and passive components, which functions with an increasingly higher cutoff frequency (f_c). The heterostructure barrier varactor (HBV) diode [1] is now a well-established device for frequency multiplying, producing signals at millimeter and sub-millimeter wavelengths. Capacitance modulation leads to the generation of odd harmonics of the applied signal frequency. Such discrete devices fabricated by the authors using an InP-based In–GaAs–InAlAs–AlAs heterostructure barrier configuration have shown an output power of 9 mW at an output frequency of 250 GHz [2]. In order to obtain a higher cutoff frequency, reducing the values of the parasitic elements of such devices/circuits via transfer-substrate (TS) and membrane-like approaches [3]–[7] have become promising. For an HBV diode, these elements are characterized by the parasitic capacitance (C_p) and the series resistance (R_s). We have previously shown that the fabrication of air-bridge connected HBV devices on quartz substrate, following a TS procedure, demonstrates a significantly reduced value of C_p [8] with respect to devices fabricated on InP substrate.

In this letter, we monolithically integrate such devices together with passive components in order to form ready-to-use

Manuscript received January 3, 2002; revised May 21, 2002. This work was supported by the Centre National d'Etudes Spatiales (CNES). The review of this letter was arranged by Associate Editor Dr. Arvind Sharma.

T. David, S. Arscott, T. Akalin, and D. Lippens are with the Institut d'Électronique et de Microélectronique du Nord (IEMN), Université des Sciences et Technologies de Lille, Cedex, France (e-mail: thibaut.david@iemn.univ-lille1.fr).

J.-M. Munier and G. Beaudin are with the Laboratoire d'Etudes du Rayonnement et de la Matière en Astrophysique (LERMA), Observatoire de Paris, Paris, France.

P. Mounaix is with the Centre de Physique Moléculaire Optique et Hertzienne, Université de Bordeaux, Bordeaux, France.

Publisher Item Identifier 10.1109/LMWC.2002.801935.

millimeter-wave chips, thus eliminating the necessity of the cumbersome “flip-chip” mounting stage. Fabrication is achieved via a combination of TS and epitaxial liftoff (ELO) procedures onto a quartz host substrate. State-of-the-art performances in terms of frequency capability and bandwidth are demonstrated here for HBV devices.

II. DEVICE TECHNOLOGY

A. Molecular Beam Epitaxy

A 2-in InP wafer was employed for the epitaxial growth. The HBV epitaxial layers were grown in a *Riber* gas-source MBE system. With respect to our previous work, a triple barrier scheme instead of a double barrier was used here, composing of three $\text{In}_{0.52}\text{Al}_{0.48}\text{As}$ (50 Å)–AlAs (30 Å)– $\text{In}_{0.52}\text{Al}_{0.48}\text{As}$ (50 Å) barriers lying between $\text{In}_{0.53}\text{Ga}_{0.47}\text{As}$ (2000 Å) cladding layers doped to $N_d = 2 \times 10^{17} \text{ cm}^{-3}$. The narrow band-gap of the InGaAs cladding layers is advantageous at high frequencies, notably by reducing saturation current effects at moderate doping levels. In addition, the doping density of the n^+ $\text{In}_{0.53}\text{Ga}_{0.47}\text{As}$ ohmic contacting layers was $N_d = 1 \times 10^{19} \text{ cm}^{-3}$ for this study in an effort to further reduce R_s .

B. Device Fabrication

The TS process developed by the authors [7] has been employed to transfer a $\frac{1}{4}$ wafer of the 2-in diameter InP-based epitaxial layer onto a 1-in square quartz host wafer (400 μm). A selective etch solution (HCl:H₂O), which has a very high selectivity ratio between InGaAs and InP, was used in order to remove the InP parent substrate (350 μm). After complete removal of the InP, device processing was performed. The air-bridge connected HBV diodes were fabricated using the standard planar topological scheme. Four types of device configurations were incorporated into the mask-set for the small and large signal measurements: coaxial-type (active device area ($A = 314 \mu\text{m}^2$)), air-bridge connected coplanar-type ($A = 12 - 40 \mu\text{m}^2$, single-mesa), discrete air-bridge connected devices ($A = 12 - 40 \mu\text{m}^2$, single and double-mesa), and fully integrated monolithic circuits incorporating passive components and active air-bridge connected devices ($A = 12 - 40 \mu\text{m}^2$, single- and double-mesa) for direct mounting into a multiplier block.

Fig. 1 shows a scanning electron micrograph of a typical monolithic circuit incorporating an HBV air-bridge connected active device together with input/output antennas and a seven-section Tchebyscheff low-pass filter. The passive networks were designed and optimized using HFSS *Ansoft*. The inset to Fig. 1

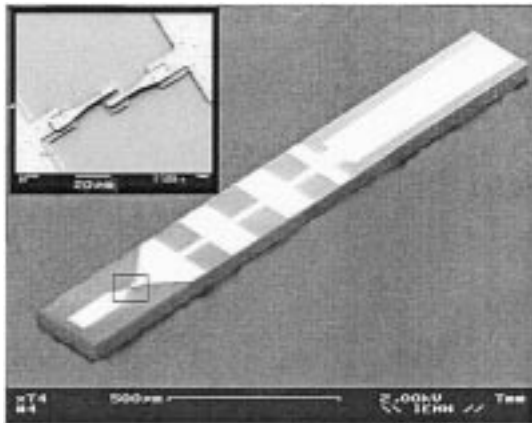


Fig. 1. Scanning electron micrograph of a monolithic circuit. Inset shows a SEM zoom of the integrated double-mesa active device ($2 \times 40 \mu\text{m}^2$).

shows a SEM close-up of the active device, the mesa area of the diode shown is $40 \mu\text{m}^2$ in a double mesa configuration (denoted as $2 \times 40 \mu\text{m}^2$ forthwith).

The upper ohmic contacts were formed using a sequential Ni–Ge–Au–Ti–Au–Ti e-beam lithography/metallization/liftoff scheme which served as a mask for the reactive ion etching (RIE) (Ar:H₂:CH₄) of the mesas. A carefully controlled RIE etch down to the n⁺ InGaAs was performed in order to reveal the bottom contacting layer for all devices. The lower ohmic contact/antenna/filter metallization was then patterned via photolithography/metallization/liftoff (Ni–Ge–Au–Ti–Au). The ohmic contacts were then alloyed using a rapid thermal annealing (400 °C/40 s). The air-bridge contacts were fabricated using a three-stage controlled dose e-beam lithography technique in order to form a mold in a PMMA/COPOLYMER e-beam resist bilayer for a Ti–Au liftoff metallization. In order to dice the individual chips, top surface pre-cutting and wafer lapping techniques were used to thin the fused quartz host wafer to 75 μm eliminating possible substrate modeing problems encountered during millimeter wave operation.

III. DEVICE CHARACTERIZATION

A. DC and Small Signal RF Characteristics

Small-signal RF measurements were carried out on the basis of s-parameter analysis using an HP Vector Network Analyzer (VNA) over the frequency range 500 MHz to 100 GHz. The RF measurements were conducted on devices which had been fabricated in coplanar-type ($12\text{--}40 \mu\text{m}^2$) and coaxial-type configurations ($A = 314 \mu\text{m}^2$).

Fig. 2 shows a family of C(V) curves as a function of diode area for air-bridge connected three-barrier single-mesa devices in coplanar layout measured at 4 GHz. It is clear that a highly symmetrical, nonlinear C(V) curve is preserved even for a small area diode ($12 \mu\text{m}^2$), both symmetry and nonlinearity being fundamental electrical characteristics for efficient odd-harmonic frequency generation. A zero-bias capacitance value of around $1 \text{ fF}/\mu\text{m}^2$, i.e., $3 \text{ fF}/\mu\text{m}^2/\text{barrier}$, is observed for all devices, whereas at an applied bias of $\pm 8 \text{ V}$ the capacitance of the smallest device ($12 \mu\text{m}^2$) is seen to fall off to a value of 7 fF, this equates to a capacitance ratio (C_{\max}/C_{\min}) of around

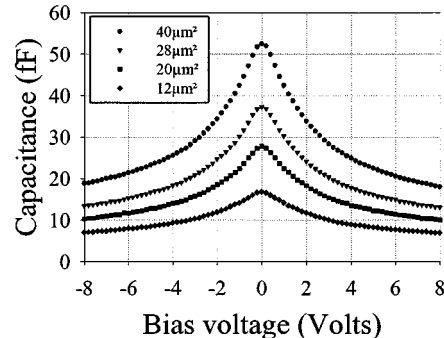


Fig. 2. Measured family of small-signal C(V) curves of discrete air-bridge connected single-mesa coplanar devices ($A = 12 - 40 \mu\text{m}^2$) at 4 GHz.

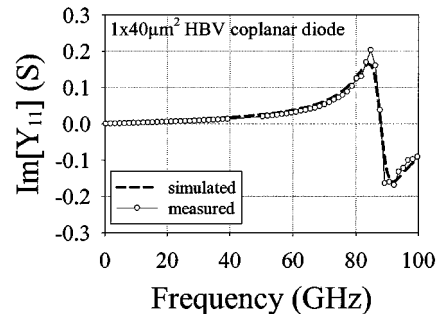


Fig. 3. Small-signal variations of the imaginary part of the admittance of a coplanar-type device ($A = 40 \mu\text{m}^2$), simulated data (dashed line), and measured data (open circles).

4:1 when C_p is taken into account. This agrees well with C(V) measurements on large surface coaxial-type devices.

These very low capacitance levels can be explained by: 1) the epitaxial staking of three barriers in series and 2) the low dielectric constant of the quartz host wafer leading to a reduced value of parasitic capacitance. The value of C_p was evaluated to be of the order of 4–5 fF by lumped element analysis using microwave design system (MDS), in good agreement with our past observations [8].

Fig. 3 shows the simulated and measured variations of the imaginary part of the admittance at zero-bias for a single-mesa HBV diode having an area of $40 \mu\text{m}^2$. The resonance at 88 GHz is due to the presence of the interconnecting inductive air-bridge element (L_p), around 60 pH, and enables thus, accurate determination of lumped elements.

B. Large-Signal Millimeter-Wave Measurements

The large-signal measurements have been conducted at the Observatoire de Paris. An existing multiplier block [2] incorporating E and H plane tuners on both the input and output circuits has been used. Input and output waveguides are orthogonal, the input guide being WR-10 (75–110 GHz), and the output guide WR-3 (220–325 GHz). High-performance tunable short-circuits are used to provide the matching. The results presented here were obtained with a $12-\mu\text{m}^2$ diode in a double-mesa configuration.

The experimental setup consists of a carcinotron can be tuned at W-band with a relatively high output power, up to 110 mW at selected frequencies. The up-converted power was measured by means of an Anritsu power meter, which had been previously

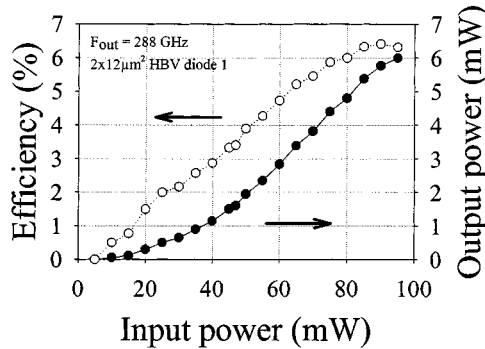


Fig. 4. Large-signal characteristics at an output frequency of 288 GHz for a monolithic circuit incorporating a double-mesa $12\text{-}\mu\text{m}^2$ HBV diode.

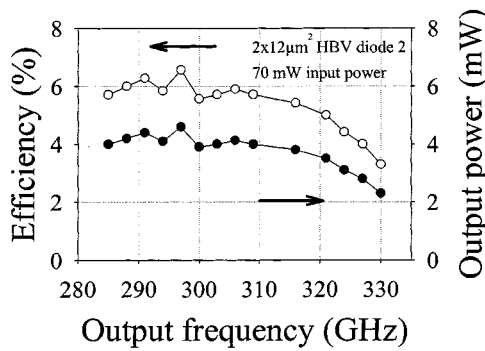


Fig. 5. Variation of the output power and efficiency versus measured output frequency at a constant input power of 70 mW for a monolithic circuit incorporating a double-mesa $12\text{-}\mu\text{m}^2$ HBV diode.

calibrated using a Thomas Keating absolute power meter. Fig. 4 shows the variation of the output power and overall efficiency as a function of the input power. A maximum output power of 6 mW was obtained at an input frequency of 96 GHz, i.e., a tripled output frequency of 288 GHz, this corresponds to an overall efficiency of around 6%. Fig. 5 shows the output power and efficiency of a $12 \mu\text{m}^2$ diode in a double-mesa configuration as a function of the measured output frequency at a constant input power of 70 mW. Optimum impedance matching was found at each frequency by using the input and output tuners. It can be seen that sizable output powers are available up to 330 GHz, corresponding to a 45-Hz (15%) 3-dB bandwidth for a central output frequency of around 300 GHz.

IV. CONCLUSION

We have demonstrated transfer-substrate and epitaxial liftoff techniques to be very powerful for the fabrication of ready-to-use millimeter-wave integrated circuits combine InP-based heterostructure barrier varactor diodes and passive components. Such a circuit incorporating a $12\text{-}\mu\text{m}^2$ double-mesa HBV diode has produced an output power of 6 mW at a frequency of 288 GHz together with a 45-GHz (15%) bandwidth and significant output powers up to 330 GHz. We are currently exploring new device topologies that take advantage of the buried metal layer technologies developed by the authors in order to further reduce the parasitic components of such devices and their related circuitry.

ACKNOWLEDGMENT

The authors would like to thank E. Delos (IEMN) and B. Lecomte (Observatoire de Paris) for their technical assistance during the small- and large-signal RF characterization. In addition, they would like to thank F. Mollot (IEMN) for the expert growth of the epitaxial layers.

REFERENCES

- [1] E. L. Kollberg and A. Rydberg, "Quantum-barrier-varactor diode for high efficiency millimeter-wave multiplier," *Electron. Lett.*, vol. 25, pp. 1696–1697, 1989.
- [2] X. Mélique, A. Maestrini, M. Favreau, O. Vanbésien, J. M. Goutoule, G. Beaudin, T. Nähr, and D. Lippens, "Record performances of a 250 GHz InP based heterostructure barrier varactor tripler," *Electron. Lett.*, vol. 35, p. 938, 1999.
- [3] R. Meola, J. Freyer, and M. Claassen, "Improved frequency tripler with integrated single barrier," *Electron. Lett.*, vol. 36, pp. 803–804, 2000.
- [4] Q. Lee, S. C. Martin, D. Mensa, R. P. Smith, J. Guthrie, and M. J. W. Rodwell, "Submicron transferred-substrate heterojunction bipolar transistors," *IEEE Electron Device Lett.*, vol. 20, pp. 396–398, Aug. 1999.
- [5] P. H. Siegel, R. P. Smith, M. C. Gaidis, and S. C. Martin, "2.5 THz GaAs monolithic membrane-diode mixer," *IEEE Trans. Microwave Theory Tech.*, vol. 47, pp. 596–604, May 1999.
- [6] I. Mehdi, S. M. Marazita, D. A. Humphrey, T.-H. Lee, R. J. Dengler, J. E. Oswald, A. J. Pease, S. C. Martin, W. L. Bishop, T. W. Crowe, and P. H. Siegel, "Improved 240 GHz subharmonically pumped planar schottky diode mixers for space-borne applications," *IEEE Trans. Microwave Theory Tech.*, vol. 46, pp. 2036–2042, 1998.
- [7] S. Arscott, P. Mounaix, and D. Lippens, "Substrate transfer process for InP-based heterostructure barrier varactor devices," *J. Vac. Sci. Technol. B*, vol. 18, pp. 150–155, Jan. 2000.
- [8] S. Arscott, T. David, X. Mélique, P. Mounaix, O. Vanbésien, and D. Lippens, "Transferred-substrate InP-based heterostructure barrier varactor diodes on quartz," *IEEE Microwave Guided Wave Lett.*, vol. 10, pp. 472–474, Nov. 2000.